

NOTICE: This is the author's version of a work that was accepted for publication in Precambrian Research. Changes resulting from the publishing process, such as peer review, editing, corrections, structural formatting, and other quality control mechanisms may not be reflected in this document. Changes may have been made to this work since it was submitted for publication. A definitive version was subsequently published in Precambrian Research, Vol. 231 (2013). doi: 10.1016/j.precamres.2013.04.007

Elsevier Editorial System(tm) for Precambrian Research
Manuscript Draft

Manuscript Number: PRECAM3647R1

Title: Paleomagnetism of Cryogenian Kitoi mafic dykes in South Siberia: implications for Neoproterozoic paleogeography

Article Type: Research Paper

Keywords: Siberian Craton, Neoproterozoic, mafic dykes, paleomagnetism, Rodinia, Cryogenian

Corresponding Author: Dr. Sergei A. Pisarevsky, PhD

Corresponding Author's Institution: University of Western Australia

First Author: Sergei A. Pisarevsky, PhD

Order of Authors: Sergei A. Pisarevsky, PhD; Dmitry P Gladkochub, DSc; Konstantine M Konstantinov, PhD; Anatoly M Mazukabzov; Arcady M Stanevich; Brendan Murphy, PhD; Jennifer A Tait, PhD; Tatiana V Donskaya, DSc; Innokentiy K Konstantinov

Abstract: We present a new paleomagnetic pole of 1.1°N , 22.4°E , $A95=7.4^{\circ}$ from the 760 Ma gabbro-dolerite Kitoi dykes located in the southern part of the Siberian Craton. The pole is supported by contact tests and suggests closer position of Siberia relative to Laurentia at 760 Ma than in Mesoproterozoic. We propose that this closer configuration was achieved by dextral transpressive motion of Siberia relative to Laurentia between 780 and 760 Ma. This motion was probably initiated at the first stage of the Rodinia breakup and is coeval with the 780 Ma Gunbarrel magmatic event of the western Canadian shield.

Abstract

We present a new paleomagnetic pole of 1.1°N , 22.4°E , $A_{95}=7.4^{\circ}$ from the 760 Ma gabbro-dolerite Kitoi dykes located in the southern part of the Siberian Craton. The pole is supported by contact tests and suggests closer position of Siberia relative to Laurentia at 760 Ma than in Mesoproterozoic. We propose that this closer configuration was achieved by dextral transpressive motion of Siberia relative to Laurentia between 780 and 760 Ma. This motion was probably initiated at the first stage of the Rodinia breakup and is coeval with the 780 Ma Gunbarrel magmatic event of the western Canadian shield.

1 Palaeomagnetism of Cryogenian Kitoi mafic dykes in South Siberia: implications 2 for Neoproterozoic paleogeography

3

4 Sergei A. Pisarevsky^{a,b,c,*}, Dmitry P. Gladkochub^d, Konstantine M. Konstantinov^d,5 Anatoly M. Mazukabzov^d, Arkady M. Stanevich^d, J. Brendan Murphy^e, Jennifer A.6 Tait^a, Tatiana V. Donskaya^d, Innokenty K. Konstantinov^d

7

8 ^a *The Grant Institute, University of Edinburgh, King's Buildings, Edinburgh, UK,*9 *EH9 3JW*10 ^b *ARC Centre of Excellence for Core to Crust Fluid Systems (CCFS) and The Institute*11 *for Geoscience Research (TIGeR), Department of Applied Geology, Curtin*12 *University, GPO Box U1987, Perth, WA 6845, Australia.*13 ^c *School of Earth and Environment, University of Western Australia, 35 Stirling*14 *Highway, Crawley, WA 6009, Australia*15 ^d *Institute of the Earth's Crust, Siberian Branch of the Russian Academy of Sciences,*16 *128 Lermontov Str., Irkutsk 664033, Russia*17 ^e *Department of Earth Sciences, St. Francis Xavier University, Antigonish, NS B2G*18 *2W5, Canada*

19

20 **Abstract**

21 We present a new paleomagnetic pole of 1.1°N, 22.4°E, A₉₅=7.4 ° from the 760 Ma

22 gabbro-dolerite Kitoi dykes located in the southern part of the Siberian Craton. The

23 pole is supported by contact tests and suggests closer position of Siberia relative to

24 Laurentia at 760 Ma than in Mesoproterozoic. We propose that this closer

25 configuration was achieved by dextral transpressive motion of Siberia relative to

26 Laurentia between 780 and 760 Ma. This motion was probably initiated at the first

27 stage of the Rodinia breakup and is coeval with the 780 Ma Gunbarrel magmatic
28 event of the western Canadian shield.

29 *Keywords:* Siberian Craton, Neoproterozoic, mafic dykes, paleomagnetism, Rodinia,
30 Cryogenian.

31 * Corresponding author: Sergei.Pisarevsky@uwa.edu.au

32

33 **1. Introduction**

34 According to most Neoproterozoic paleogeographic models, the Rodinia
35 supercontinent finally amalgamated at 1000-900 Ma and started to break up at 800-
36 750 Ma, although the exact timing of these events and the precise configuration of
37 Rodinia are controversial (e.g., Hoffman, 1991; Dalziel, 1997; Pisarevsky et al., 2003;
38 Li et al., 2008). The role and place of Siberia in these events is a key part of this long-
39 lasting controversy. Most workers suggest that Siberia was juxtaposed with the
40 northern margin of Laurentia controversy (e.g., Hoffman, 1991; Condie and Rosen,
41 1994; Frost et al., 1998; Rainbird et al., 1998; Pisarevsky et al., 2008; but see Sears
42 and Price, 2000), but a more precise reconstruction is hindered by the lack of early
43 and middle Neoproterozoic paleomagnetic data.

44 Although reliable ca. 1500-1450 Ma and ca. 1050-950 Ma paleomagnetic data
45 from Siberia and Laurentia (Table 2; see also Pavlov, 1994; Ernst et al., 2002;
46 Veselovsky et al., 2006) support coherent movement of these two continents during
47 most of Mesoproterozoic, they also suggest a paleolatitudinal separation, implying the
48 presence of some other continental block(s) in between (Wingate et al., 2009). The
49 apparent absence of any exposures of the giant 1267 Ma Mackenzie igneous event in
50 Siberia supports this inference (Gladkochub et al., 2006a, b; Pisarevsky et al., 2008).
51 However, the 710-730 Ma mafic igneous rocks along the southern margin of Siberia
52 (Neimark et al., 1990; Rytisk et al., 2002; Ernst et al., 2012) may be related to the
53 Laurentian 723 Ma Franklin giant igneous event. If so, at ca. 720 Ma Siberia may

54 have been closer to Laurentia than it was in Mesoproterozoic, a hypothesis that would
55 have major implications for Neoproterozoic reconstructions and for models of
56 Rodinia breakup. Some reliable ca.790-720 Ma paleomagnetic data from both
57 continents are therefore needed to test this hypothesis. Sklyarov et al. (2003) reported
58 a 743 ± 47 Ma Sm–Nd isochron age and a 758 ± 4 Ma ^{40}Ar - ^{39}Ar plateau age for mafic
59 dykes along the Kitoi river in the Sharyzhalgai massif of the southern Siberia (Fig. 1)
60 which may be related to the Franklin event. A pilot study of these dykes
61 (Konstantinov, 2006) demonstrated the presence of a stable paleomagnetic
62 remanence. In this paper we present results of a 2009 field study in which we carried
63 out a detailed paleomagnetic sampling of the Kitoi dykes with the purpose of
64 obtaining a highly reliable Cryogenian paleomagnetic pole for Siberia.

65

66 **2. Geology and sampling.**

67 The Siberian craton (Fig. 1a) is a Paleoproterozoic collage of mostly Archean
68 granulite-gneiss and granite-greenstone complexes (Rosen et al., 2005) surrounded by
69 major Phanerozoic suture zones (Zonenshain et al., 1990; Parfenov, 1991). The
70 basement is exposed only in two shields, Aldan-Stanovoy and Anabar, and in some
71 outcrops of the Olenek (north), Kan, Biryusa, Sharyzhalgai, and Baikal (south-west)
72 inliers (Fig. 1; Gladkochub et al., 2006a).

73 Several Proterozoic mafic dyke swarms and some associated sills are located
74 along the western shore of Lake Baikal and at the basement inlier of the Archean
75 Tungus superterrane, known as the Sharyzhalgai metamorphic massif (Fig. 1a). The
76 Sharyzhalgai massif is composed of Archean tonalite-trondhjemite-granodiorite
77 (TTG) series, Archean and Paleoproterozoic granite-gneisses, metavolcanic and
78 metasedimentary rocks, including granulites. These rocks are intruded by ca. 2530 Ma
79 Kitoi granitoids (Gladkochub et al., 2005) and ca. 1850 – 1870 Ma Sayan and
80 Shumikha granites (Donskaya et al., 2002; Levitskii et al., 2002; Didenko et al., 2003;

81 Poller et al., 2004). Most of the Sharyzhalgai massif, including our study area, is
82 located far from the Main Sayan Fault and from the Baikal rift, so no tilting or block
83 rotations related to Phanerozoic tectonism occurred here. Mafic intrusions of two
84 different magmatic episodes have been described (Sklyarov et al., 2003).

85 Dykes related to the first magmatic episode are rare. They are composed of
86 medium grained sub-alkaline gabbro-dolerites that are sub-vertical in orientation
87 (Sklyarov et al., 2003; Gladkochub et al., in press). These dykes are slightly deformed
88 and metamorphosed, containing minerals typical of greenschist facies. One of these
89 dykes has been recently dated at 1864 ± 4 Ma by U-Pb (zircon, TIMS; Gladkochub et
90 al., in press).

91 The dykes (or sheets) associated with the second episode are abundant in the
92 Sharyzhalgai massif. These dykes are commonly 1.5-3.0 m wide, shallowly ($25-35^\circ$)
93 dipping to SW, and are composed mostly of unaltered fine-grained gabbro-dolerite of
94 tholeiitic composition (Fig. 1b; Sklyarov et al., 2003). Some of the dykes can be
95 mapped up to 7–8 km in length, but aeromagnetic data suggest that individual dykes
96 may attain a length of 12–15 km (Sklyarov et al., 2003). Similarities in mineralogy,
97 geochemistry, petrology and structural orientation (Sklyarov et al., 2003) suggest that
98 these dykes are coeval and are derived from a single mantle source. One of these
99 dykes (K5, Fig.1) was dated at 758 ± 4 Ma ($^{40}\text{Ar}-^{39}\text{Ar}$, plagioclase) and 743 ± 47 Ma
100 (Sm-Nd, whole rock-mineral) by Sklyarov et al. (2003) and these data suggest a ca.
101 760 Ma age for the intrusions.

102 In 2009 we collected paleomagnetic samples from eleven Sharyzhalgai ca. 760
103 Ma shallow-dipping dykes and from two vertical Late Paleoproterozoic (episode 1)
104 dykes in outcrops along the Kitoi River. Cross-cutting relationships between older and
105 younger dykes were observed in one location (Fig.1b) which was sampled for the
106 paleomagnetic bake contact test. In total we collected 178 oriented cores from 13

107 dykes and host rocks. Both solar and magnetic compasses were used to determine the
108 orientation.

109

110 **3. Analytical methods**

111 Remanence behaviour was determined by detailed stepwise alternating field
112 (AF) demagnetisation (≤ 20 steps, up to 100 mT), using an AGICO LDA-3A
113 tumbling demagnetiser and the 2G cryogenic magnetometer in the University of
114 Edinburgh. Thermal stepwise demagnetisation (≤ 20 steps, to 600°C), using a
115 Magnetic Measurements MMTD1 furnace was also applied. Magnetic mineralogy
116 was investigated from demagnetisation characteristics and, in selected samples, from
117 measuring the variation of susceptibility versus temperature (20 to 700°C) using the
118 AGICO Kappabridge MFK-FA with the CS3 apparatus. Parts of the collection were
119 studied in the paleomagnetic laboratory of Utrecht University (Netherlands).
120 Magnetisation vectors were isolated using Principal Component Analysis (Kirschvink
121 1980).

122 All minerals were analysed using a modified MAR-3 microprobe in the
123 Geological Institute SB RAS (Ulan-Ude) using standard conditions of analysis
124 (operators Karmanov and Kanakin). See Table 1 of Sklyarov et al. (2003) for details.

125

126 **4. Magnetic mineralogy and rock magnetism**

127 Microprobe studies of ca. 760 Ma dykes indicate the presence of mostly
128 homogeneous titanomagnetite in the Cryogenian gabbro-dolerites (Sklyarov et al.,
129 2003). This observation is supported by magnetic susceptibility versus temperature
130 curves (Fig. 2a) Curie temperatures are distributed between 500° and 570°C,
131 which corresponds to a titanium-poor titanomagnetite $\text{Fe}_{3-x}\text{Ti}_x\text{O}_4$ with $x \approx 0.05-0.10$
132 (Fig. 3.11 in Dunlop and Özdemir, 1997). Konstantinov (2006) reached similar
133 conclusions in his preliminary studies of these dykes using differential

134 thermomagnetic analysis (DTA) and analyses of coercivity spectra. Hopkinson peaks
135 (Fig. 2) indicate the presence of paleomagnetically highly stable single-domain (SD)
136 or pseudo-single-domain (PSD) grains.

137 The 1864 Ma vertical dykes show similar distribution of Curie temperatures
138 also indicating SD or PSD titanium-poor titanomagnetite (Fig.2b) and DTA analyses
139 led to the same conclusion (Konstantinov, 2006).

140

141 **5. Paleomagnetic analysis**

142 *5.1. 760 Ma dykes*

143 The intensity of the natural remanent magnetization (NRM) of Cryogenian
144 gabbro-dolerites ranges from 20 mA/m to 2.5 A/m, and their magnetic susceptibility
145 from ~ 2 to 90×10^{-4} SI units. After removal of a low-stability, randomly oriented
146 overprint, thermal (Fig. 3a), AF demagnetisations (Fig. 3b) and a combination of both
147 (Fig. 3c) of the Cryogenian gabbro-dolerites reveal a stable shallow eastward unipolar
148 characteristic magnetisation ChRM. Unblocking temperatures are in most cases
149 between 550 and 590°C typical for the titanium-poor titanomagnetite and magnetite.
150 The relatively high coercivities of these gabbro-dolerites are indicative of SD or PSD
151 titanomagnetite and magnetite - typically 60 to 100 mT was required for the AF
152 demagnetization (Fig.3b). Mean ChRM directions for each dyke are shown in Table 1
153 (entries 1-11). Remanence directions from all dykes, except for K9, show reasonably
154 well grouping with $\alpha_{95} < 16^\circ$. The mean direction for ten dykes (dyke K9 was
155 excluded) is: $D = 80.8^\circ$, $I = -12.1^\circ$, $k = 42.8$, $\alpha_{95} = 7.8^\circ$. The corresponding
156 paleomagnetic pole of 1.1°N , 21.8°E ($A_{95}=7.4^\circ$) falls far from any younger Siberian
157 paleopole (McElhinny and Lock, 1996; Smethurst et al., 1998; Pisarevsky, 2005;
158 Shatsillo and Pavlov, 2006; Metelkin et al., 2012), suggesting that the ChRM of
159 studied gabbro-dolerites is primary.

160 *5.2. Paleoproterozoic dykes*

161 The remanence of nearly vertical Paleoproterozoic dykes is also stable (Fig.
162 4a), but its directions are rather scattered (Table 1) and vary significantly from dyke
163 to dyke (Table 1; Fig.5b). The K4 dyke is exposed only near the contact of the cross-
164 cutting 760 Ma K3 dyke. The remanence directions of all (except two) K4 samples
165 are similar to the remanence direction of the K3 dyke. The remanence directions of
166 dykes K6 and K7 apparently represent two geomagnetic polarities, but the mean
167 directions are not antipodal (Table 1). This disparity may reflect either a significant
168 time difference in their magnetisations, or a high level of geomagnetic secular
169 variations. In either case the corresponding paleopoles (entries 14-16 in Table 1)
170 should be considered as Virtual Geomagnetic Poles (VGPs), which may reflect
171 positions of geomagnetic rather than geographic pole at the time of the dyke's
172 emplacement.

173

174 **6. Contact tests**

175 We collected ten samples from the 1864 Ma dyke K4 within 102 cm from its
176 contact with the shallow dipping 760 Ma dyke K3. Eight of these samples were
177 collected within 70 cm from the contact and yield the remanence direction similar to
178 the mean remanence direction of dyke K3 (Table 1, entry 12; Fig. 4b; Fig. 5a), shown
179 as a star in Fig. 5. However, the remanence directions of two K4 samples collected at
180 >70 cm from the contact are steeper and are close to the inverted mean direction for
181 another 1865 Ma dyke K7. We tentatively interpret these data to provide a positive
182 contact test and evidence for the primary remanences of both sets of dykes.

183 We collected fourteen samples from host gneisses within 1 m from dykes K3,
184 K5, K8, K9, K12, K13 and K14 and thirty one samples from host gneisses far from
185 their contacts with dykes. Half of the unbaked gneiss samples are paleomagnetically
186 unstable, but the other half yield a scattered bipolar remanence (Table 1, entry 17;
187 Fig. 4c; Fig. 5b). After an inversion of downward directions, this remanence has a

188 loose grouping with a mean direction of $D=13^\circ$, $I=-67^\circ$ ($\alpha_{95}=24^\circ$). The age of this
189 remanence is unclear, but its direction is significantly different from that of the 760
190 Ma dykes (Table 1; Fig.5b). All baked rocks yield stable remanence close to that of
191 the 760 Ma dykes (Table 1, entry 13; Fig. 4d; Fig. 5b). We interpret these data as
192 evidence for the primary remanence of 760 Ma dykes, but cannot classify it as the full
193 positive contact test because of the scattered remanence of the unbaked host rocks.

194

195 **7. Discussion**

196 Our new 760 Ma paleomagnetic pole suggests an equatorial position of the
197 Siberian craton rotated by about 90° clockwise compare to its present-day orientation.
198 This pole provides a test for published Neoproterozoic continental reconstructions.
199 Most of these reconstructions imply contiguity between Siberia and Laurentia during
200 at least some part of the Proterozoic, but the precise configuration and timing have
201 been widely debated (e.g. Hoffman, 1991; Condie and Rosen, 1994; Frost et al., 1998;
202 Rainbird et al., 1998; Sears and Price, 2000; Gallet et al., 2000; Pisarevsky and
203 Natapov, 2003; Gladkochub et al., 2006b; Pisarevsky et al., 2008; Wingate et al.,
204 2009). Paleomagnetic tests (Pisarevsky and Natapov, 2003; Pisarevsky et al., 2008)
205 indicate that (i) reconstructions with ‘tight’ fit between Laurentia and Siberia
206 (Hoffman, 1991; Condie and Rosen, 1994; Frost et al., 1998; Rainbird et al., 1998;
207 Sears and Price, 2000) are not supported by 1050-950 Ma paleomagnetic data and (ii)
208 Laurentia and Siberia could have moved coherently during that time only if Siberia
209 has been located NW of Laurentia with significant ‘gap’ between them that was
210 presumably occupied by some yet unknown piece(s) of the continental crust. Possibly
211 those pieces included some fragments of Arctic Alaska (Rainbird et al., 1996).

212 Wingate et al. (2009) reported a new ca 1475 Ma Siberian paleomagnetic pole.
213 This pole together with coeval Laurentian pole of Meert and Stuckey (2002) suggest
214 that the distant position of Siberia with respect to Laurentia may be valid between ca.

215 1500 and 1000 Ma. This distant relationship might explain an apparent absence of any
216 traces of the giant 1267 Ma Mackenzie igneous event in Siberia (Gladkochub et al.,
217 2006b; Pisarevsky et al., 2008).

218 Notably, these hypotheses assume that Siberian craton behaved as a rigid coherent
219 continent since Mesoproterozoic to present time. Gurevich (1984) analysed Early
220 Paleozoic Siberian paleomagnetic data and suggested that there was a significant
221 mismatch between poles from SW Siberia (Aldan block) and poles from NW Siberia
222 (Anabar-Angara block), which implies a clockwise rotation between two blocks
223 during the opening of the v-shaped Vilyui syncline in Devonian times. Pavlov et al.
224 (2008) provided more geophysical, geological and paleomagnetic evidence for such
225 rotation and reported the best estimation of Euler rotation parameters. Using these
226 parameters we modified the shape of the pre-Devonian Siberia (figs. 6-8). This
227 restoration also caused the rotation of ca. 1050-950 Ma Siberian poles (Pavlov et al.,
228 2000, 2002; Gallet et al., 2000) from the Aldan block (Table 2). These readjustments
229 provide a tighter fit of ca. 1500-950 Ma coeval Siberian and Laurentian poles, but still
230 require a distant position of Siberia with respect to Laurentia (Fig. 6).

231 There are no reliable ca. 760 Ma Laurentian poles (Table 2), but the closeness
232 of precisely dated 778 ± 2 Ma Tzesotene Sills (TS) and Gunbarrell Dykes (GD) poles
233 to precisely dated $723^{+4/-2}$ Ma Franklin Dykes (FD) pole and less precisely dated
234 Uinta Formation (UF) pole (Table 2) suggest a little movement of Laurentia between
235 ca. 780-720 Ma. Hence we reconstructed the ca. 760 Ma position of Siberia and
236 Laurentia using our new Kitoi pole and the middle point between Laurentian 778 ± 2
237 Ma and $723^{+4/-2}$ Ma poles (Tables 1 and 2; Fig. 7). This reconstruction implies that
238 after ca. 1000 Ma Siberia obliquely moved closer to Laurentia to its new position at
239 760 Ma (Fig. 7). The exact timing of this movement is not constrained. However, it
240 could be associated with the 780 Ma Gunbarrell magmatic event (Harlan et

241 al., 2003) which reflects rifting along the western margin of Laurentia (e.g., Hoffman,
242 1999; Powell et al., 1994) and the first stage in the breakup of Rodinia (Li et al., 2008
243 and references therein).

244 Our paleomagnetic data suggest that modifications to recently published
245 Neoproterozoic reconstructions are required to accommodate the oblique (clockwise)
246 convergence of Siberia relative to Laurentia in addition to the separation of
247 Australia/South China from Laurentia (Li et al., 2008). Taken together, these relative
248 motions require that Siberia, Laurentia and Australia/South China are on three
249 different plates, implying the existence of a triple point between them. Fig. 8 shows a
250 possible scenario for this event, one which can be tested against the tectonothermal
251 evolution of several adjacent continental blocks. The approximately orthogonal
252 separation of Australia/South China from both Laurentia and Siberia suggests that the
253 plate boundaries between them were oceanic ridges. However, the oblique
254 convergence between Laurentia and Siberia implied by the paleomagnetic data
255 suggests that the plate boundary between these continents was a transform fault that
256 accommodated the relative dextral (clockwise) motion between them.

257 The scenario presented in Figure 8 implies nearly orthogonal convergence
258 between Baltica and Siberia, implying the existence of a subduction zone between
259 them. However, the arc that may record this convergence has not been identified. As
260 the leading edge of Siberia has no record of arc magmatism, we place Siberia on the
261 lower plate, although it is possible that an unknown continental block may have been
262 positioned between Siberia and Baltica in which case the polarity of subduction is
263 unclear.

264 The new, closer position of Siberia and Laurentia suggests that some traces of
265 the giant ca. 723 Ma Franklin magmatic event might occur in southern Siberia. There
266 were no ca. 723 Ma magmatic bodies reported from southern Siberia until recently.
267 However, Ernst et al. (2012) published a ca. 725 Ma age (U-Pb, ID-TIMS,

268 baddeleyite) of the Dovyren pluton in the Baikal-Patom margin of the Siberian craton
269 (Fig. 1). On the other hand, to our knowledge, no igneous rocks coeval to ca. 760-740
270 Ma Biryusa sills (Gladkochub et al., 2006) and Kitoi dykes (Sklyarov et al., 2003)
271 were reported from northern Laurentia. The latter can be explained either by the local
272 extend of the ca. 760-740 Ma magmatism in southern Siberia, or by a passing of
273 Siberia-Laurentia system over the mantle plume between ca. 760 Ma (causing some
274 minor magmatism in southern Siberia) and 725 Ma, eventually causing the giant
275 Franklin magmatic event, involved the southern margin of Siberia (725 Ma Dovyren
276 pluton, Ernst et al., 2012) (Fig. 8). The data used by Sklyarov et al. (2003) to define
277 the Sm-Nd isochron for the ca. 760 Ma mafic dykes yield $\epsilon_{\text{Nd}}(t)$ values ranging from
278 -3.5 to -3.9, suggesting the dykes were derived from an enriched subcontinental
279 mantle (EM1) source characterized by time-integrated depletion of Sm relative to Nd
280 (e.g. Bell and Simonetti, 1996). This signature contrasts with the more radiogenic
281 signature of the Franklin dykes (e.g. Shellnutt et al., 2004), an evolution that might
282 reflect a stronger asthenospheric component to plume-related magmatism with time.
283 In both scenarios the Franklin magmatic pulse could cause a new rifting along the
284 Arctic margin of Laurentia (Rainbird, 1993). We suggest that this rifting caused an
285 opening of the Paleo-Asian Ocean and a dramatic change in the movement of Siberia,
286 eventually resulting in almost 180° rotation of Siberia by the Early Cambrian, as
287 indicated by abundant, but not always precisely dated Ediacaran and Cambrian
288 paleomagnetic data from Siberia (e.g. Kirschvink and Rozanov, 1984; Pisarevsky et
289 al., 2000, 1997; Pavlov and Gallet, 1998; Gallet et al., 2003; Shatsillo and Pavlov,
290 2006; Pavlov et al., 2008 and references therein). The ca. 720 Ma Franklin magmatic
291 event could have increased of the speed of Siberia away from the plume and slowed
292 down or even reversed the movement of Laurentia, a scenario analogous to the
293 process started by the Réunion plume at 60-55 Ma (Cande and Stegman, 2011).
294 Franklin plume activity may have resulted in the fan-like opening of the Palaeo-Asian

295 Ocean and initiated the clockwise rotation of Siberia. Details of this rotation are
296 beyond the scope of this study and will be published elsewhere.

297

298 **8. Conclusions**

299 According to our analysis the relative movement between Laurentia and
300 Siberia could occur during the first stage of the breakup of Rodinia between 0.80 and
301 0.75 Ga, which amalgamated at ca. 1.0 Ga. We propose that the dextral transpressive
302 motion of Siberia relative to Laurentia between 0.78 and 0.76 Ga implied in Fig. 8
303 may be indirectly related to the rifting along the western Laurentian margin (Fig. 8).
304 This motion also may cause subduction and strike-slip motions between Siberia,
305 Greenland and Baltica, but corresponding arc complexes have not yet been identified.

306

307 **Acknowledgments**

308 We thank two anonymous reviewers for their important comments which
309 improved the manuscript. Paleogeographic reconstructions are made with free
310 GPLATES software (<http://www.gplates.org/>). This is contribution 302 from the ARC
311 Centre of Excellence for Core to Crust Fluid Systems and TIGeR publication #454.
312 SP and JT gratefully acknowledge funding from the Marie Curie FP6 Excellence
313 Grant scheme and JMB acknowledges the continuing support of Natural Sciences and
314 Engineering Research Council of Canada. This research was partly supported by the
315 RFBS (Russian Foundation for Basic Research) grant 13-05-91173 and by the
316 Siberian Branch of the Russian Academy of Sciences (Earth Science Department)
317 grant 10.3.

318

319 **References**

320 Bell, K., Simonetti, A., 1996. Carbonatite magmatism and plume activity:
321 implications from the Nd, Pb and Sr isotope systematics of Oldoinyo Lengai. *Journal*
322 *of Petrology* 37, 1321–1339.

323 Bleeker, W., 2002. Achaean tectonics: A review, with illustrations from the Slave
324 craton. In: Fowler, C.M.R., Ebinger, C.J., Hawkesworth, C.J. (eds.), *The Early*
325 *Earth: Physical, Chemical and Biological Development*. Geological Society of
326 London Special Publication 199, 151–181.

327 Cande, S.C., Stegman, D.R., 2011. Indian and African plate motions driven
328 by the push force of the Reunion plume head. *Nature* 475, 47-52.

329 Condie, K. C., Rosen, O. M., 1994. Laurentia-Siberia connection revisited. *Geology*
330 22, 168-170.

331 Dalziel, I.W.D., 1997. Neoproterozoic-Paleozoic geography and tectonics: review,
332 hypothesis, environmental speculation. *Geological Society of America Bulletin* 109,
333 16-42.

334 Davis, D.W., Paces, J.B., 1990. Time resolution of geologic events on the Keweenaw
335 Peninsula and applications for development of the Midcontinent Rift system. *Earth*
336 *and Planetary Science Letters* 97, 54-64.

337 Denyszyn, S.W., Halls, H.C., Davis, D.W., Evans, D.A.D., 2009. Paleomagnetism
338 and U-Pb geochronology of Franklin dykes in High Arctic Canada and Greenland: a
339 revised age and paleomagnetic pole constraining block rotations in the Nares Strait
340 region. *Canadian Journal of Earth Sciences* 46, 689-705.

341 Didenko, A.N., Kozakov, I.K., Bibikova, E.V., Vodovozov, V.Y., Khil'tova, V.Y.,
342 Reznitskii, L.Z., Ivanov, A.V., Levitskii, V.I., Travin, A.V., Shevchenko, D.O.,
343 Rasskazov, S.V., 2003. Paleoproterozoic granites of the Sharyzhalgai block, Siberian
344 Craton: Paleomagnetism and geodynamic inferences. *Doklady Earth Sciences* 390,
345 510-515.

346 Diehl, J.F., Haig, T.D., 1994. A paleomagnetic study of the lava flows within the
347 Copper Harbour Conglomerate, Michigan: new results and implications. *Canadian*
348 *Journal of Earth Sciences* 31, 369-380.

349 Donskaya, T.V., Sal'nikova, E.B., Sklyarov, E.V., Gladkochub, D.P., Mazukabzov,
350 A.M., Kovach, V.P., Yakovleva, S.Z., Berezhnaya, N.G., 2002. Early proterozoic
351 postcollision magmatism at the southern flank of the Siberian Craton: New
352 geochronological data and geodynamic implications. *Doklady Earth Sciences* 383,
353 125-128.

354 Dunlop, D.J., Özdemir, Ö., 1997. *Rock Magnetism; Fundamentals and Frontiers*.
355 *Cambridge Studies in Magnetism* 3. Cambridge University Press, Cambridge, 573 p.

356 Ernst, R.E., Hamilton, M.A., Soderlund, U., 2012. A proposed 725 Ma Dovyren-
357 Kingash LIP of southern Siberia, and possible reconstruction link with the 725-715
358 Ma Franklin LIP of northern Laurentia. Abstract volume 35, Geological Association
359 of Canada (GAC) – Mineralogical Association of Canada (MAC) Joint Annual
360 Meeting – Geoscience at the Edge, May 27-29, 2012, St. John's, Newfoundland and
361 Labrador, Canada.

362 Ernst, R.E., Buchan, K.L., Hamilton, M.A., Okrugin, A.V., Tomshin, M.D., 2000.
363 Integrated paleomagnetism and U–Pb geochronology of mafic dikes of the Eastern
364 Anabar shield region, Siberia: implications for Mesoproterozoic paleolatitude of
365 Siberia and comparison with Laurentia. *Journal of Geology* 108, 381–401.

366 Frost, B.R., Avchenko, O.V., Chamberlain, K.R., Frost, C.D., 1998. Evidence for
367 extensive Proterozoic remobilization of the Aldan Shield and implications for
368 Proterozoic plate tectonic reconstructions of Siberia and Laurentia. *Precamb. Res.* 89,
369 1-23.

370 Gallet, Y., Pavlov, V.E., Semikhatov, M.A., Petrov, P.Yu., 2000. Late
371 Mesoproterozoic magnetostratigraphic results from Siberia: paleogeographic

372 implications and magnetic field behaviour. *Journal of Geophysical Research* 105,
373 16481-16499.

374 Gallet, Y., Pavlov, V., Courtillot, V., 2003. Magnetic reversal frequency and
375 Apparent Polar Path of the Siberian platform in the earliest Paleozoic, inferred from
376 the Khorbusuonka river section (northeastern Siberia). *Geophysical Journal*
377 *International* 154, 829–840.

378 Gladkochub et al., in press. First evidence of the Paleoproterozoic mafic post-
379 collisional magmatism in the Pre-Sayan basement inlier in south Siberia. *Doklady*
380 *RAN*.

381 Gladkochub, D.P., Donskaya, T.V., Mazukabzov, A.M., Sal'nikova, E.B., Sklyarov,
382 E.V., Yakovleva, S.Z., 2005. The age and geodynamic interpretation of the Kitoi
383 granitoid complex (southern Siberian craton). *Russian Geology and Geophysics*
384 46(11), 1121-1133.

385 Gladkochub, D., Pisarevsky, S.A., Donskaya, T., Natapov, L.M., Mazukabzov, A.,
386 Stanevich, A.M., Sklyarov, E., 2006a. Siberian Craton and its evolution in terms of
387 Rodinia hypothesis. *Episodes* 29, 169–174.

388 Gladkochub, D.P., Wingate, M.T.D., Pisarevsky, S.A., Donskaya, T.V., Mazukabzov,
389 A.M., Ponomarchuk, V.A., Stanevich, A.M., 2006b. Mafic intrusions in southwestern
390 Siberia and implications for a Neoproterozoic connection with Laurentia. *Precambrian*
391 *Research* 147, 260-278.

392 Gladkochub, D., Donskaya, T., Wingate, M.T.D, Poller, U., Kröner, A., Fedorovsky,
393 V., Mazukabzov, A., Todt, W., Pisarevsky, S.A., 2008. Petrology, geochronology,
394 and tectonic implications of c. 500 Ma metamorphic and igneous rocks along the
395 northern margin of the Central-Asian Orogen (Olkhon terrane, Lake Baikal, Siberia).
396 *Journal of the Geological Society London* 165 (1), 235-246.

397 Gurevich, E.L., 1984. Paleomagnetism of the Ordovician deposits of the Moyero river

398 sequence. Paleomagnetic methods in stratigraphy. VNIGRI, St. Petersburg, pp. 35–41
399 (in Russian).

400 Harlan, S.S., Geissman, J.W., Snee, L.W., 1997. Paleomagnetic and $^{40}\text{Ar}/^{39}\text{Ar}$
401 geochronologic data from late Proterozoic mafic dykes and sills, Montana and
402 Wyoming. USGS Professional Paper 1580, 16 pp.

403 Harlan, S.S., Heaman, L., LeCheminant, A.N., Premo, W.R., 2003. Gunbarrel
404 mafic magmatic event: a key 780 Ma time marker for Rodinia plate reconstructions.
405 *Geology* 31, 1053–1056.

406 Henry, S.G., Mauk, F.J., Van der Voo, R., 1977. Paleomagnetism of the upper
407 Keweenawan sediments: the Nonesuch Shale and Freda Sandstone. *Canadian Journal*
408 *of Earth Sciences* 14, 1128-1138.

409 Hoffman, P. F., 1991. Did the breakout of Laurentia turn Gondwanaland inside-out?
410 *Science* 252, 1409-1412.

411 Kirschvink, J. L. 1980. The least squares line and plane and the analysis of
412 palaeomagnetic data. *Geophysical Journal of the Royal Astronomic Society* 62, 699 –
413 718.

414 Kirschvink, J.L., Rozanov, A.Yu., 1984. Magnetostratigraphy of lower Cambrian
415 strata from the Siberian Platform: a palaeomagnetic pole and a preliminary polarity
416 time-scale. *Geological Magazine* 121, 189-203.

417 Konstantinov, K.M., 2006. Paleomagnetic characteristics of Nersinsk gabbro-dolerites
418 in the Sharyzhalgai salient. In: Sklyarov, E.V. (Ed), *Precambrian evolution of*
419 *southern part of the Siberian craton*. Novosibirsk, Publishing House of the Siberian
420 Branch of the Russian Academy of Sciences, pp.310-317.

421 Levitskii, V.I., Mel'nikov, A.I., Reznitskii, L.Z., Bibikova, E.V., Kirnozova, T.I.,
422 Kozakov, I.K., Makarov, V.A., Plotkina, Y.V., 2002. Early Proterozoic postcollisional
423 granitoids in southwestern Siberian craton. *Geologiya i geofizika* 43, 717-731.

424 Li, Z.X., Bogdanova, S.V., Collins, A., Davidson, A., De Waele, B., Ernst, R.E.,
425 Fitzsimons, I., Fuck, R., Gladkochub, D., Jacobs, J., Karlstrom, K., Lu, S., Milesi, J-
426 P., Myers, J., Natapov, L., Pandit, M., Pease, V., Pisarevsky, S.A., Thrane, K.,
427 Vernikovsky, V., 2008. Assembly, configuration, and break-up history of Rodinia: a
428 synthesis. *Precambrian Research* 160, 179-210.

429 McCabe, C., Van der Voo, R., 1983. Paleomagnetic results from the upper
430 Keweenawan Chequamegon Sandstone: implications for red bed diagenesis and Late
431 Precambrian apparent polar wander of North America. *Canadian Journal of Earth
432 Sciences* 20, 105-112.

433 McElhinny, M.W., Lock, J. 1996. IAGA paleomagnetic databases with Access.
434 *Surveys in Geophysics* 17(5), 575–591. doi:10.1007/BF01888979.

435 Meert, J.G., Stuckey, W., 2002 Revisiting the paleomagnetism of the 1.476 Ga
436 St.Francois Mountains igneous province, Missouri, *Tectonics* 21,1007,
437 doi:10.1029/2000TC001265.

438 Metelkin, D.V., Vernikovsky, V.A., Kazansky, A.Yu., 2012. Tectonic evolution of
439 the Siberian paleocontinent from the Neoproterozoic to the Late Mesozoic:
440 paleomagnetic record and reconstructions. *Russian Geology and Geophysics* 53, 675–
441 688.

442 Müller, R. D., Gaina. C., Roest, W.R., Hansen, D.L., 2002. A recipe for
443 microcontinent formation. *Geology* 29(3), 203–206.

444 Neimark, L.A., Rytsk, E.Yu., Levchenkov, O.A., Komarov, A.N., Yakovleva, S.Z.,
445 Nemchin, A.A., Shuleshko, I.K., Korikovskiy, S.P., 1990. The Early Proterozoic-
446 Upper Riphean age of rocks of the Olokit complex (northern Cisbaikalia) according to
447 data of zircon geochronology. In: Shemyakin, V.M. (ed), *The geology and
448 geochronology of the Precambrian of the Siberian Platform and its framing*, 206–222,
449 Nauka, Leningrad (in Russian).

450 Ovchinnikova, G.V., Semikhatov, M.A., Vasil'eva, I.M., Gorokhov, I.M., Kaurova,
451 O.K., Podkovyrov, V.N., Gorokhovskii, B.M., 2001. Pb–Pb age of limestones of the
452 middle Riphean Malgina Formation, the Uchur –Maya region of East Siberia.
453 *Stratigraphy and Geological Correlation* 9, 490–502.

454 Parfenov, L.M., 1991. Tectonics of the Verkhoyansk-Kolyma Mesozoides in the
455 context of plate tectonics. *Tectonophysics* 199, 319–342.

456 Park, J.K., Norris, D.K., Larochele, A., 1989. Paleomagnetism and the origin of the
457 Mackenzie Arc of northwestern Canada. *Canadian Journal of Earth Sciences* 26,
458 2194-2203.

459 Pavlov, V.E., 1994. Paleomagnetic poles from the Uchur-Maya Riphean
460 hypostratotype and Riphean drift of the Aldan block of the Siberian Platform.
461 *Doklady Academy of Science* 336(4), 533-537 (in Russian).

462 Pavlov, V., Gallet, Y., 1998. Upper Cambrian to Middle Ordovician
463 magnetostratigraphy from the Kulumbe river section (northwestern Siberia). *Physics*
464 *of the Earth and Planetary Interiors* 108, 49–59.

465 Pavlov, V.E., Gallet, Y., Shatsillo, A.V., 2000. Palaeomagnetism of the upper
466 Riphean Lakhanda Group of the Uchur–Maya area and the hypothesis of the late
467 Proterozoic supercontinent. *Fizika Zemli* 8, 23– 34 (in Russian).

468 Pavlov, V.E., Gallet, Y., Petrov, P.Yu., Zhuravlev, D.Z., Shatsillo, A.V., 2002. Uy
469 series and late Riphean sills of the Uchur –Maya area: isotopic and palaeomagnetic
470 data and the problem of the Rodinia supercontinent. *Geotectonics* 36, 278– 292.

471 Pavlov, V.E., Bachtadse, V., Mikhailov, V., 2008. New Middle Cambrian and Middle
472 Ordovician palaeomagnetic data from Siberia: Llandelian magnetostratigraphy and
473 relative rotation between the Aldan and Anabar–Angara blocks. *Earth and Planetary*
474 *Science Letters* 276, 229–242.

475 Pisarevsky, S.A., 2005. New edition of the global palaeomagnetic database.
476 *EOS Transactions, American Geophysical Union*, 86, 170.

477 Pisarevsky, S.A., Natapov, L.M., 2003. Siberia and Rodinia. *Tectonophysics* 375,
478 221-245. DOI:10.1016/j.tecto.2003.06.001

479 Pisarevsky, S.A., Gurevich, E.L., Khramov, A.N., 1997. Palaeomagnetism of the
480 Lower Cambrian sediments from the Olenek river section (northern Siberia):
481 paleopoles and a problem of magnetic polarity in Early Cambrian. *Geophysical*
482 *Journal International*, 130, 746-756.

483 Pisarevsky, S.A., Komissarova, R.A., Khramov, A.N., 2000. New palaeomagnetic
484 results from Vendian red sediments in Cisbaikalia and the problem of the relationship
485 of Siberia and Laurentia in the Vendian. *Geophysical Journal International*, 140, 598-
486 610.

487 Pisarevsky, S. A., Wingate, M. T. D., Powell, C. McA., Johnson, S., Evans, D. D.,
488 2003, Models of Rodinia assembly and fragmentation. In: Yoshida M., Windley
489 B.F., (Eds.), *Proterozoic East Gondwana: Supercontinent Assembly and Breakup*.
490 Geological Society of London, Special Publications 206, 35-55.

491 Pisarevsky, S.A., Natapov, L.M., Donskaya, T.V., Gladkochub, D.P., Vernikovskiy,
492 V.A., 2008. Proterozoic Siberia: a promontory of Rodinia. *Precambrian Research* 160,
493 66–76.

494 Poller, U., Gladkochub, D.P., Donskaya, T.V., Mazukabzov, A.M., Sklyarov, E.V.,
495 Todt, W., 2004. Early Proterozoic collisional magmatism along the Southern Siberian
496 craton – constrains from U-Pb single zircon data. *Transactions of the Royal Society*
497 *Edinburgh* 152, 1116-1127.

498 Powell, C.M., Preiss, W.V., Gatehouse, C.G., Krapez, B., Li, Z.X., 1994. South
499 Australian record of a Rodinian epicontinental basin and its mid-Neoproterozoic
500 breakup (approximately 700 Ma) to form the palaeo-Pacific Ocean. *Tectonophysics*
501 237, 113–140.

502 Rainbird, R.H., 1993. The sedimentary record of mantle plume uplift preceeding
503 eruption of the Neoproterozoic Natkusiak flood basalt. *Journal of Geology* 101, 305-
504 318.

505 Rainbird, R.H., Jefferson, C.W., Young, G.M., 1996. The early Neoproterozoic
506 sedimentary Succession B of northwestern Laurentia: Correlations and
507 paleogeographic significance. *Geological Society of America Bulletin* 108, 454-470.

508 Rainbird, R.H., Stern, R.A., Khudoley, A.K., Kropachev, A.P., Heaman, L.M.,
509 Sukhorukov, V.I., 1998. U-Pb geochronology of Riphean sandstone and gabbro from
510 southeast Siberia and its bearing on the Laurentia-Siberia connection. *Earth and*
511 *Planetary Science Letters* 164, 409-420.

512 Rosen, O.M., Manakov, A.V., Serenko, V.P., 2005. Paleoproterozoic collisional
513 system and diamondiferous lithospheric keel of the Yakutian kimberlite province.
514 *Russian Geology and Geophysics* 46 (12), 1237–1251.

515 Roy, J.L., Robertson, W.A., 1978. Paleomagnetism of the Jacobsville Formation and
516 the apparent polar path for the interval ~1100 to ~670 m.y. for North America.
517 *Journal of Geophysical Research* 83, 1289-1304.

518 Rytsk, E.Yu., ShalaeV, V.S., Rizvanova, N.G., Krymskii, R.Sh., Makeev, A.F., Rile,
519 G. V., 2002. The Olokit Zone of the Baikal Fold Region: New Isotope-
520 Geochronological and Petrogeochemical Data. *Geotectonics* 36(1), 24-35.

521 Sears, J.W., Price, R.A., 2000. New look at the Siberian connection: no SWEAT.
522 *Geology* 28, 423-426.

523 Shatsillo, A.V., Pavlov, V.E., 2006. Paleomagnetism of Vendian rocks in the
524 southwest of the Siberian Platform. *Russian Journal of Earth Sciences* 7, 7, ES3006,
525 doi:10.2205/2005ES000192.

526 Shellnutt, J.G., Dostal, J., Keppie, J.D., 2004. Petrogenesis of the 723 Ma Coronation
527 sills, Amundsen basin, Arctic Canada: implications for the break-up of Rodinia.
528 *Precambrian Research*, 129, 309-324.

529 Sklyarov, E.V., Gladkochub, D.P., Mazukabzov, A.M., Menshagin, Y.V., Watanabe,
530 T., Pisarevsky, S.A., 2003. Neoproterozoic mafic dike swarms of the Sharyzhlgai
531 metamorphic massif (southern Siberian craton). *Precambrian Research* 122, 359–376.

532 Smethurst, M.A., Khramov, A.N., Torsvik, T.H., 1998. The Neoproterozoic and
533 Palaeozoic palaeomagnetic data for the Siberian Platform: From Rodinia to Pangea.
534 *Earth-Science Reviews* 43, 1-24.

535 Stanevich A.M., Mazukabzov A.M., Postnikov A.A., Nemerov V.K., Pisarevsky S.A.,
536 Gladkochub D.P., Donskaya T.V., Kornilova T.A., 2007. Northern fragment of the
537 Paleasian ocean in Neoproterozoic: sedimentation history and geodynamic
538 interpretation. *Russian Geology and Geophysics*, 48(1), 46-60.

539 Veselovsky, R.V., Gallet, Y., Pavlov, V.E., 2003. Paleomagnetism of the traps of
540 Podkamennaya Tunguska and Kotuy rivers valleys: on the question about the
541 post-Paleozoic relative motions of the Siberian and East-European platforms. *Fizika*
542 *Zemli (Solid Earth)* 39, 78–94.

543 Warnock, A.C., Kodama, K.P., Zeitler, P.K., 2000. Using thermochronometry
544 and low-temperature demagnetization to accurately date Precambrian
545 paleomagnetic poles. *Journal of Geophysical Research* 105, 19435–19453.

546 Weil, A.B., Geissman, J.W., Ashby, J.M., 2006. A new paleomagnetic pole for the
547 Neoproterozoic Uinta Mountain supergroup, Central Rocky Mountain States, USA.
548 *Precambrian Research* 147, 234-259.

549 Wingate, M.T.D., Pisarevsky, S.A., Evans, D.A.D., 2002. Rodinia connections
550 between Australia and Laurentia: no SWEAT, no AUSWUS? *Terra Nova* 14, 121-
551 128.

552 Wingate, M.T.D., Pisarevsky, S.A., Gladkochub, D.P., Donskaya, T.V., Konstantinov,
553 K.M., Mazukabzov, A.M., Stanevich, A.M., 2009. Geochronology and
554 paleomagnetism of mafic igneous rocks in the Olenek Uplift, northern Siberia:

555 implications for Mesoproterozoic supercontinents and paleogeography. *Precambrian*
556 *Research* 170, 256-266, doi: 10.1016/j.precamres.2009.01.004.
557 Zonenshain, L.P., Kuzmin, M.I., Natapov, L.M., 1990. *Geology of the USSR: A plate*
558 *tectonic synthesis*. Geodynamic Monograph. American Geophysical Union,
559 Washington, Ser. 21.

560 **Figure captions**

561 **Fig. 1.** (a) Precambrian tectonic and paleogeographic elements of the Siberian Craton;
562 (b) geology of the study area and sampling localities.

563 **Fig. 2.** Magnetic susceptibility (κ) versus temperature curves; (a) 760 Ma dyke; (b)
564 1865 Ma dyke.

565 **Fig. 3.** Demagnetisations of the 760 Ma dykes. In orthogonal plots, open (closed)
566 symbols show magnetisation vector endpoints in the vertical (horizontal) plane;
567 curves show changes in intensity during demagnetisation. Stereoplots (equal-angle
568 projection) show upwards (downwards) pointing palaeomagnetic directions with open
569 (closed) symbols; (a) thermal demagnetisation; (b) AF demagnetisation; (c)
570 combination of AF and thermal demagnetisations.

571 **Fig. 4.** Demagnetisations of the 1865 Ma dykes and country gneiss; (a) 1865 Ma dyke
572 K6; (b) 1865 Ma dyke K4, 5 cm from the contact with 760 Ma dyke K3; (c) country
573 gneiss distal from dykes; (d) country gneiss, 10 cm from 760 Ma dyke K5.

574 **Fig. 5.** Baked contact tests; (a) contact between 760 Ma dyke K3 and 1865 Ma dyke
575 K4 (squares denote mean remanence directions of the 1865 Ma dyke K6 and K7, the
576 latter is inverted); (b) remanence directions of baked and unbaked gneiss. Star denotes
577 the mean remanence direction of ten 760 Ma dykes.

578 **Fig. 6.** New paleomagnetically supported reconstruction of Laurentia and Siberia at
579 1000 Ma. Laurentia is rotated to the absolute framework about a pole at 10.32°N,
580 142.27°W by -25.33°. Siberia is rotated to Laurentia about a pole at 69.95°N,

581 133.23°E by +127.05°. Southeastern Siberia (Aldan block) is rotated to northwestern
582 Siberia about a pole at 62°N, 117°E by +23° (Pavlov et al., 2008). Acronyms for
583 paleopoles are as in Table 2.

584 **Fig. 7.** Displacement of Siberia with respect to Laurentia after 1000 Ma: (a)
585 paleogeographic reconstruction in Laurentian coordinates, at 760 Ma Siberia is
586 rotated to Laurentia about a pole at 69.66°N, 78.92°E by + 130.99° ; (b)
587 paleomagnetic poles (polar projection).

588 **Fig. 8.** 780 Ma (a), 760 Ma (b) and 725 Ma (c) reconstructions of Laurentia, Siberia,
589 South China and Australia. Rotation parameters: (a) Laurentia is rotated to the
590 absolute framework about a pole at 16.11°N, 59.52°E by +87.4°, Siberia is rotated to
591 Laurentia about a pole at 69.95°N, 133.23°E by +127.05°; (b) Laurentia is rotated to
592 absolute framework about a pole at 10.28°N, 67.42°E by +90.91°, Siberia is rotated to
593 Laurentia about a pole at 69.66°N, 78.92°E by +130.99°; (c) Laurentia is rotated to
594 absolute framework about a pole at 6.37°N, 78.52°E by +83.24°, Siberia is rotated to
595 Laurentia about a pole at 69.66°N, 78.92°E by +130.99°. Rotation parameters for
596 Australia and South China are as in Li et al. (2008).

Table 1. Paleomagnetic directions and poles, dolerite dykes, Kitoi River, South Siberia

#	Dyke	Locality	N/n	Slat (°N)	Slong (°E)	Decl. (°)	Incl. (°)	k	α_{95} (°)	Plat (°N)	Plong (°E)	D _p (°)	D _m (°)
<i>Neoproterozoic (~760 Ma) dykes</i>													
1	K1	Alangar	19/17	52°19.57'	102°50.92'	89.8	-13.6	10.6	11.5	5.3	17.2	6.0	11.7
2	K2	"	9/7	52°19.75'	102°50.56'	80.9	-35.2	15.7	15.8	9.9	31.9	10.5	18.2
3	K3	Proval	16/8	52°14.26'	102°47.72'	76.3	-12.3	15.3	14.6	-3.4	27.5	7.6	14.6
4	K5	"	11/9	"	"	80.7	0.0	26.4	10.2	-5.7	20.2	5.1	10.2
5	K8	"	13/11	52°13.99'	102°47.46'	76.8	-8.9	28.1	8.8	-4.5	26.0	4.5	8.9
6	K9*	Kholomkha	14/7	52°11.41'	102°46.54'	61.2	-12.3	9.4	20.8	-12.0	39.8	10.2	21.2
7	K10	"	6/6	"	"	83.4	3.1	36.3	11.1	-5.3	17.1	5.7	11.3
8	K11	"	8/8	"	"	81.8	-2.8	44.8	8.4	-3.9	20.1	4.2	8.4
9	K12	"	10/6	"	"	78.8	-24.8	40.3	10.7	3.5	29.5	6.2	11.5
10	K13	"	15/10	"	"	86.4	-5.5	23.0	10.3	0.0	17.3	5.2	10.3
11	K14	"	5/5	"	"	72.7	-20.5	41.4	12.0	-1.9	32.9	6.6	12.6
	Mean for 10 dykes		126/94			80.8	-12.1	39.7	7.8	1.1	22.4	A₉₅=7.4°	
<i>Baked rocks</i>													
12	K4**	"	10/8	52°14.26'	102°47.72'	83.4	-5.7	30.0	11.2	-1.2	19.1	5.6	11.2
13		Baked gneiss	14/14			82.5	1.4	18.7	9.4	-5.1	18.3	4.7	9.4
	Mean for 1-5,7-13		150/116			81.3	-10.4	42.8	6.7	0.4	21.8	A₉₅=6.1°	
<i>Paleoproterozoic (1864 Ma) dykes</i>													
14	K4 [§]	Proval	2/2	52°14.26'	102°47.72'	101.0	-51.8	-	-	31.5	26.4	-	-
15	K6	"	11/9	"	"	197.7	-44.4	13.4	14.6	60.6	249.0	11.5	18.4
16	K7	"	9/7	"	"	254.0	46.0	7.5	23.6	12.3	41.9	19.3	30.2
<i>Unbaked host rocks</i>													
17			31/15			12.9	-66.6	3.6	23.8	12.0	94.2	32.3	39.2

N/n=number of demagnetised /used samples; Slat, Slong=locality latitude and longitude; Decl, Incl =site mean declination, inclination; k =best estimate of the precision parameter of Fisher (1953); α_{95} = the semi-angle of the 95% cone of confidence; Plat, Plong = latitude, longitude of the paleopole; D_p, D_m=the semi-axes of the cone of confidence about the pole at the 95% probability level.

* excluded from the overall mean

** samples remagnetised by K3 dyke

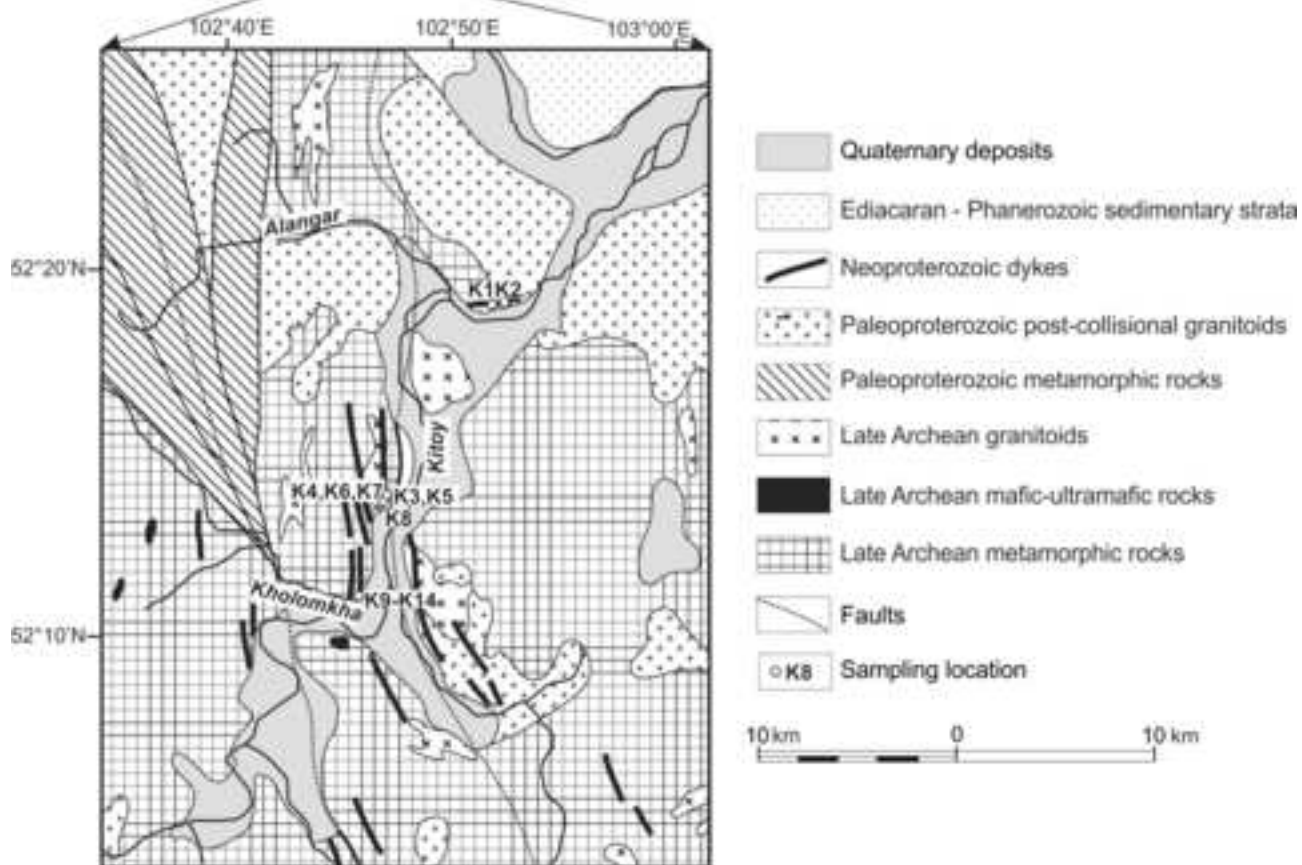
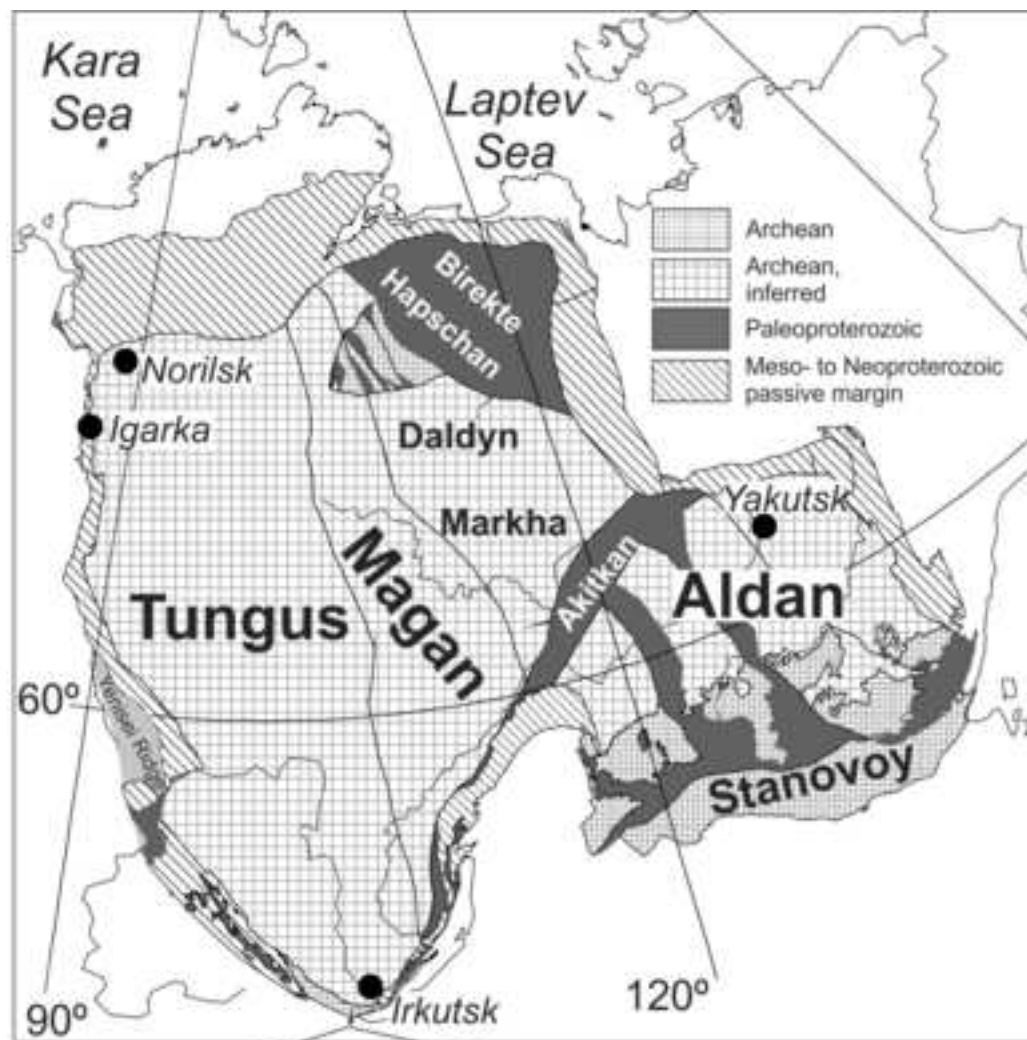
§ not remagnetised by K3 dyke

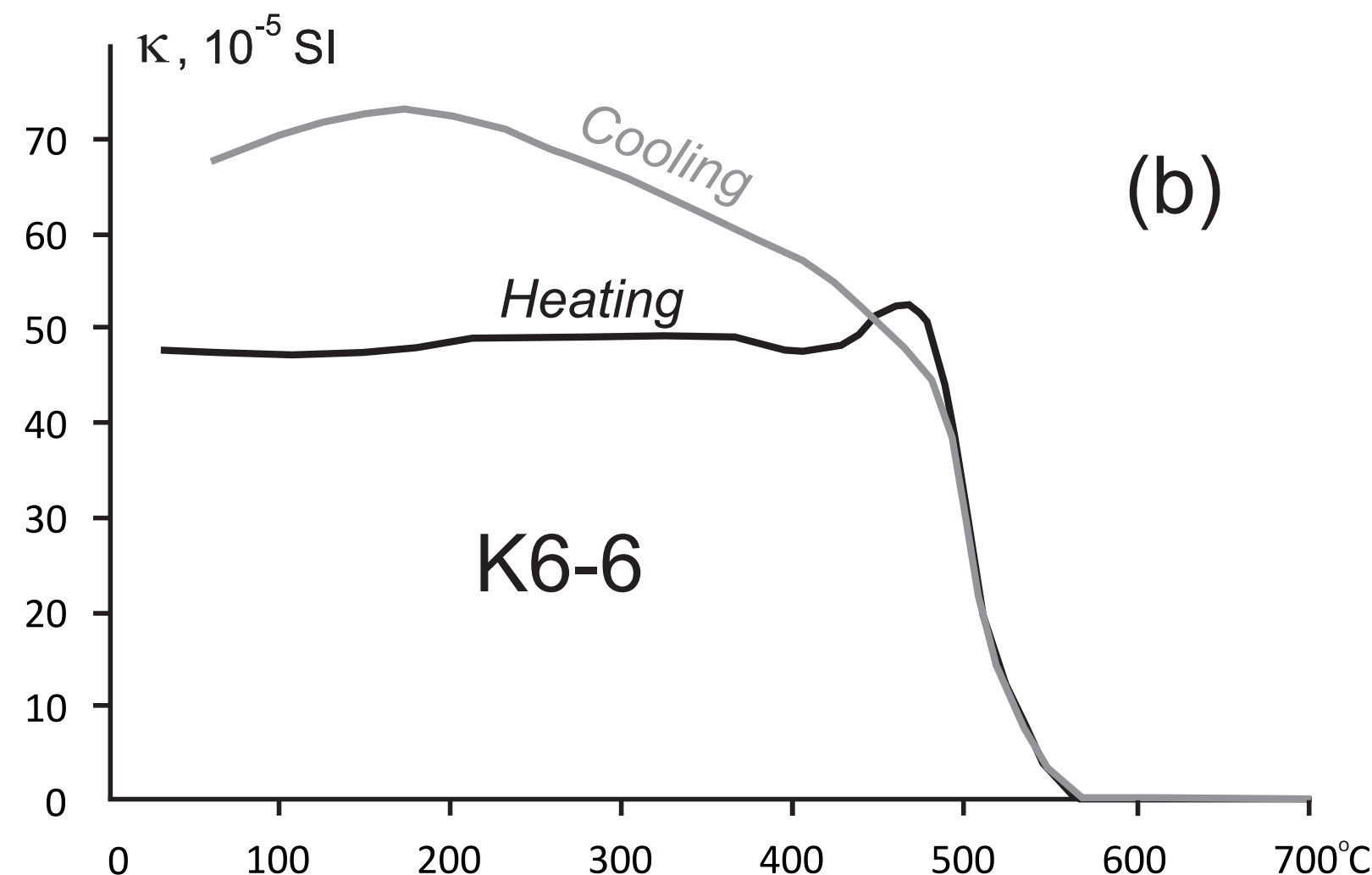
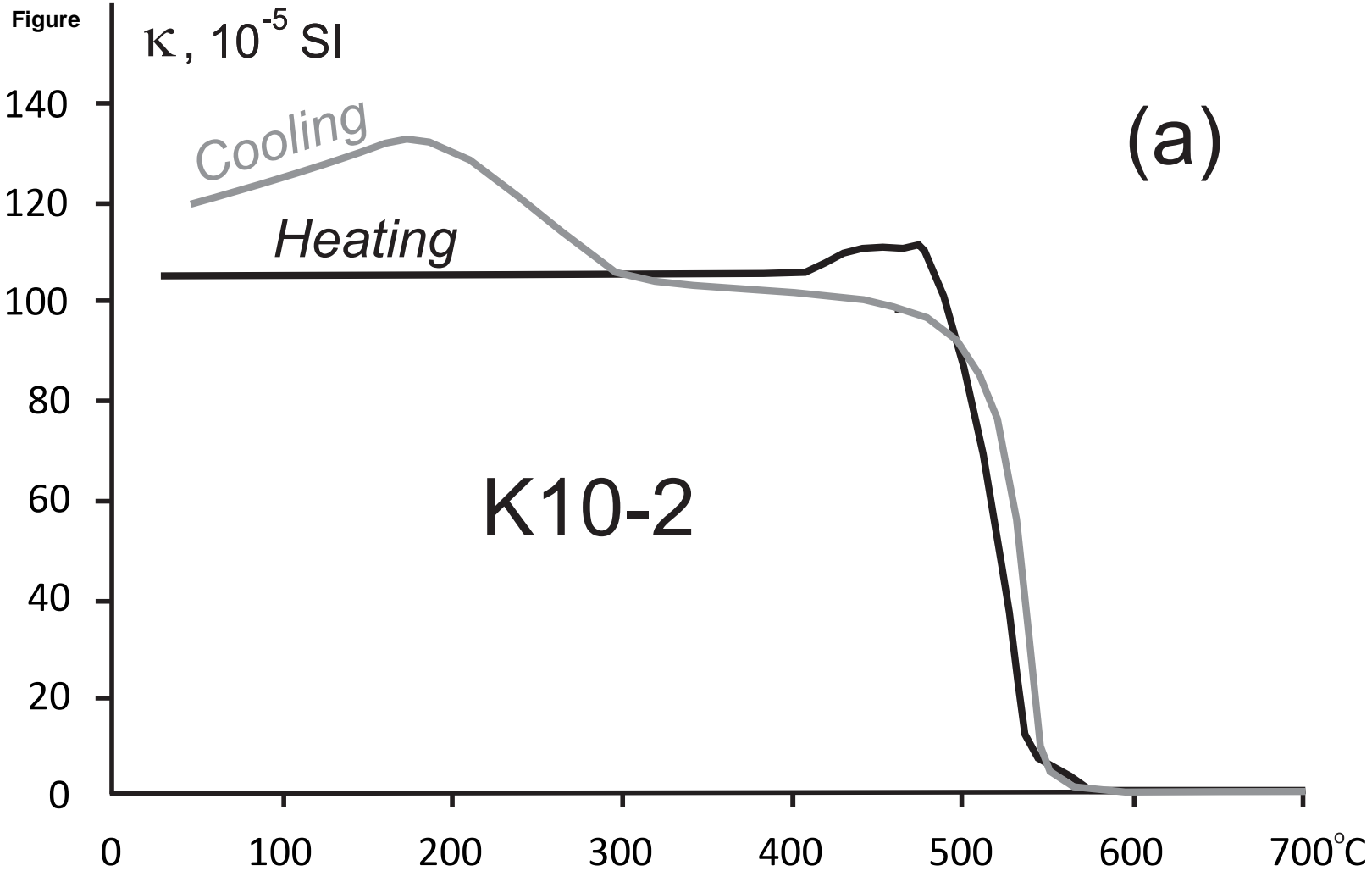
Table 2. Laurentian and Siberian ca. 1475 Ma, ca. 1080-1000 Ma and ca. 780-720 Ma palaeomagnetic poles.

#	Rockname	Age (Ma)	Plat (°N)	Plong (°E)	A ₉₅ (°)	Reference
<i>Laurentia</i>						
1	SF St.Francois Mountains	1476 ± 16	-13.2	219.0	6.1	Meert and Stuckey, 2002
2	LS Lake Shore Traps	1087 ± 2	22.2	180.8	4.5	Diehl and Haig, 1994; Davis and Paces, 1990
3	FS Freda Sandstone	1050 ± 30	2.2	179.0	4.2	Henry et al., 1977; Wingate et al., 2002
4	NS Nonesuch Shale	1050 ± 30	7.6	178.1	5.5	“
5	CS Chequamegon Sandst.	1020 ± 30	-12.3	177.7	4.6	McCabe and Van der Voo, 1983
6	JS Jacobsville Sandstone	1020 ± 30	-10.0	184.0	4.2	Roy and Robertson, 1978
7	HI Haliburton Intrusion	1030-1000	-32.6	141.9	6.3	Warnock et al., 2000
8	TS Tzesotene Sills	778 ± 2	1.6	137.8	5.0	Park et al., 1989
9	GD Gunbarrell Dykes	778 ± 2	13.9	129.4	8.2	Harlan et al., 1997
10	UF Uinta Formation	800-750	0.8	161.3	4.7	Weil et al., 2006
11	FD Franklin Dykes	723+4/-2	6.7	162.1	3.0	Denyszyn et al., 2009
<i>Siberia</i>						
12	KS Kyutingde, Sololi intrusions, Siberia	1473 ± 24	33.6	253.1	10.4	Wingate et al., 2009
13	MF Malgina Formation*	1043±14	-15.4	248.8	2.6	Gallet et al., 2000; Ovchinnikova et al., 2001
14	KF Kumakha Formation*	1040-1030	-3.2	221.4	7.0	Pavlov et al., 2000
15	MF Milkon Formation*	~1025	5.1	216.3	3.8	“
16	NF Nelkan Formation*	1025-1015	-4.4	238.8	6.3	“
17	IF Ignikan Formation*	1015-1005	-5.3	221.8	7.4	“
18	KA Kandyk Formation*	1000-950	7.0	196.7	4.3	Pavlov et al., 2002
19	UK Ust-Kirba Formation*	<KA	2.3	253.1	10.4	“
20	KD Kitoi Dykes	758 ± 4	-0.4	201.8	6.1	This study

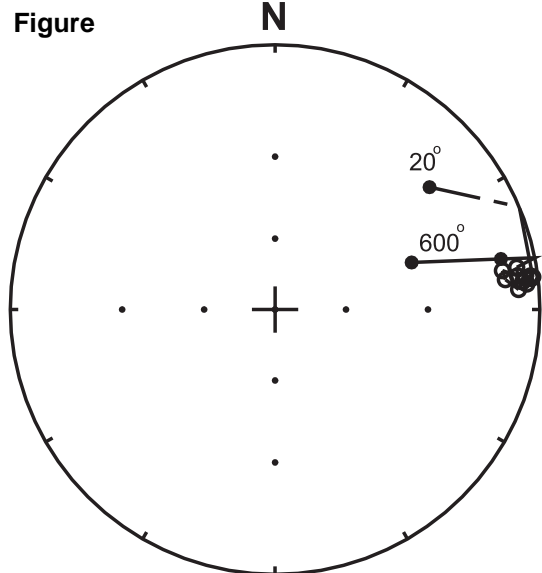
*poles rotated to NW Siberia by 23° anticlockwise, Euler's pole is 62°N, 117°E (Pavlov et al., 2008)

Figure
[Click here to download high resolution image](#)

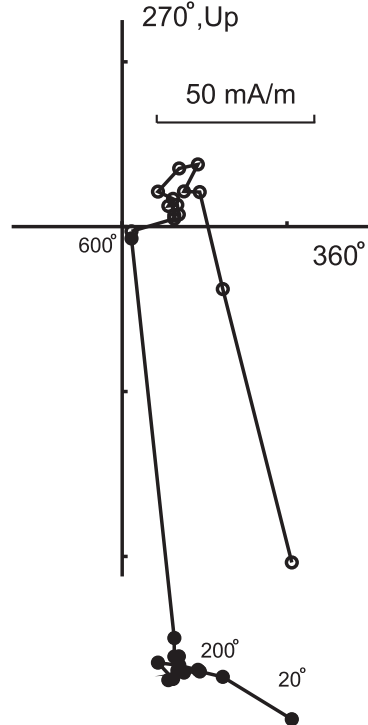
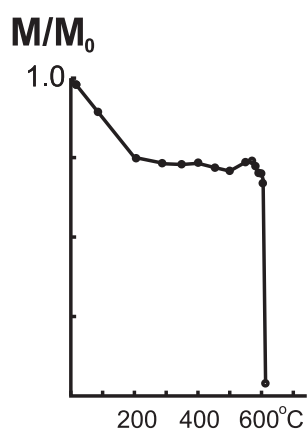




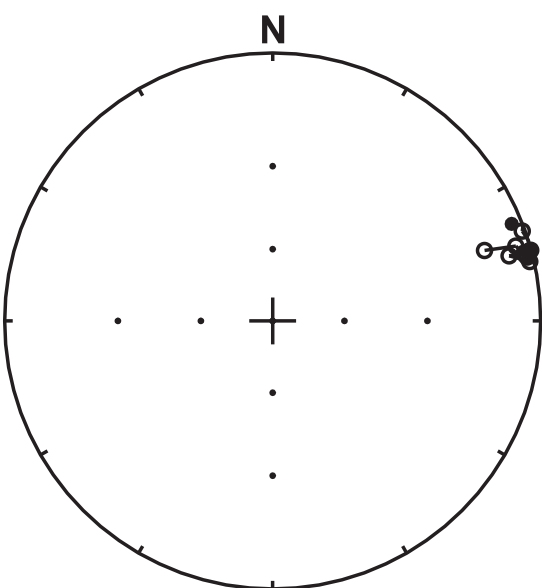
Figure



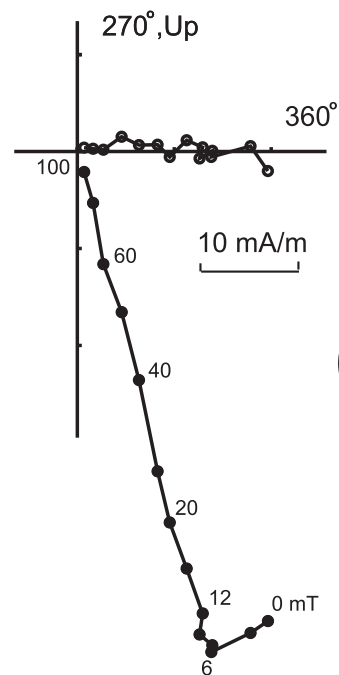
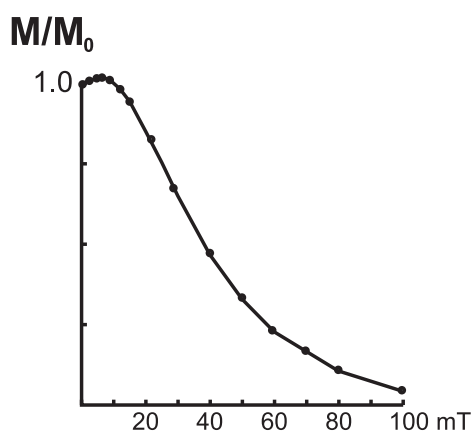
K11-3B



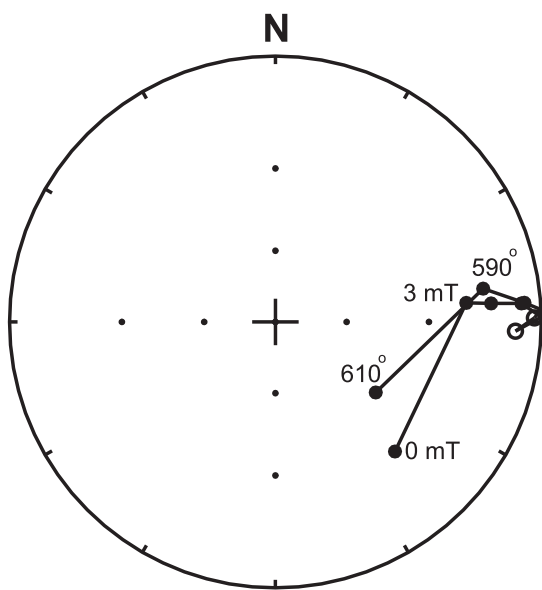
(a)



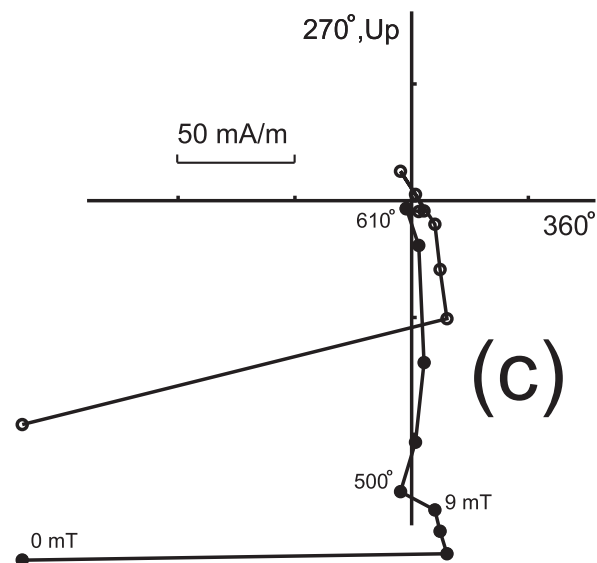
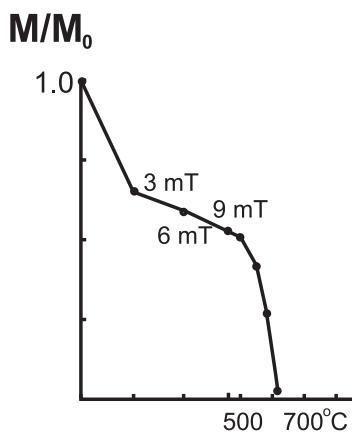
K3-7A



(b)

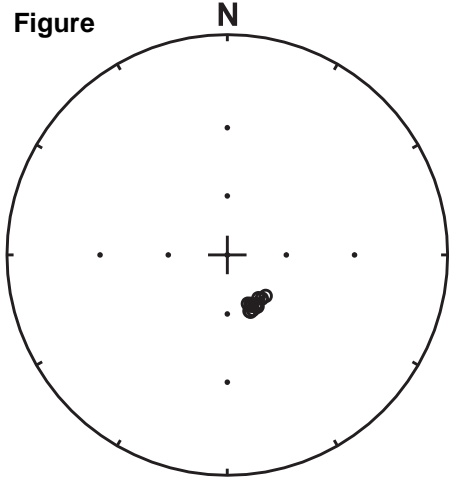


K1-17A

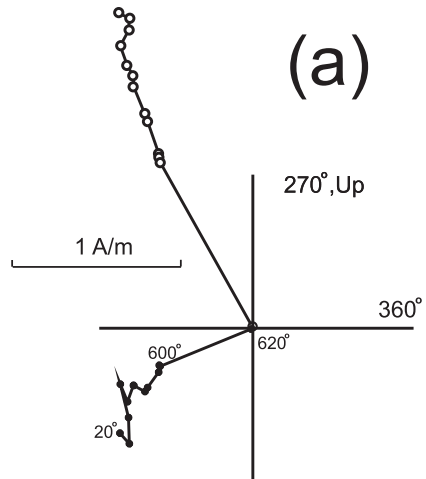
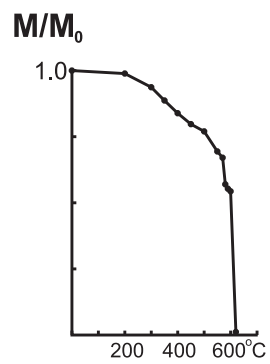


(c)

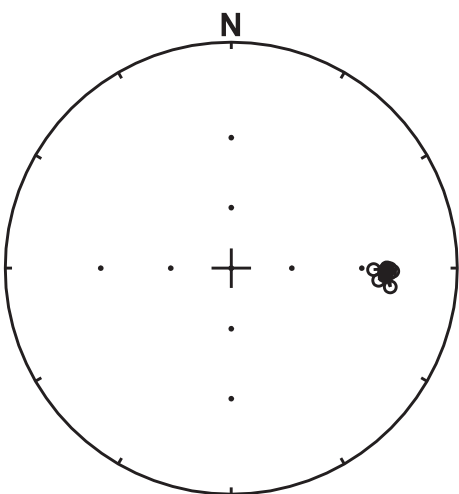
Figure



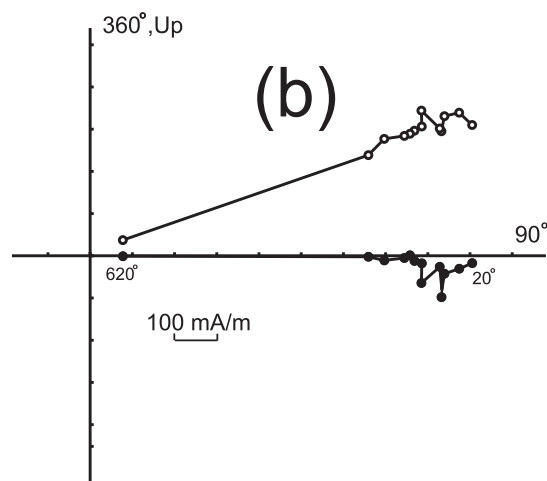
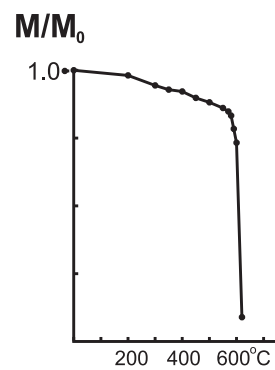
K6-6B



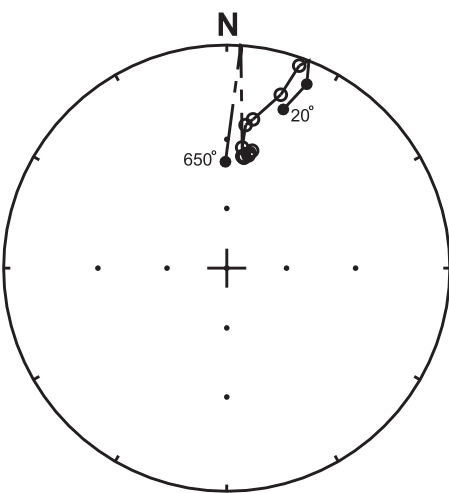
(a)



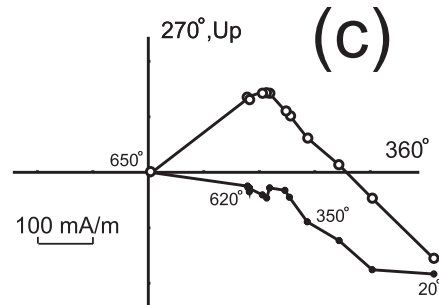
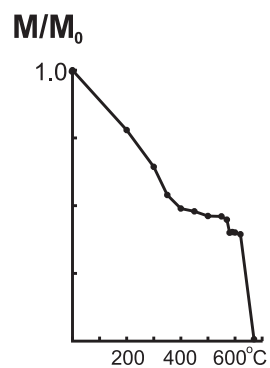
K4-1B



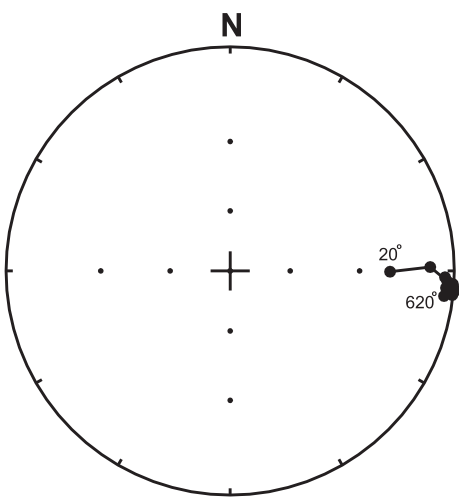
(b)



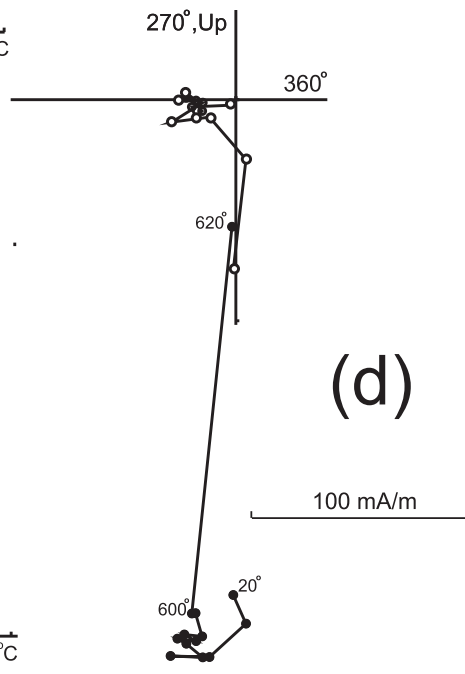
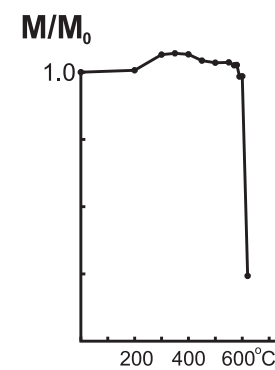
K1-6B



(c)

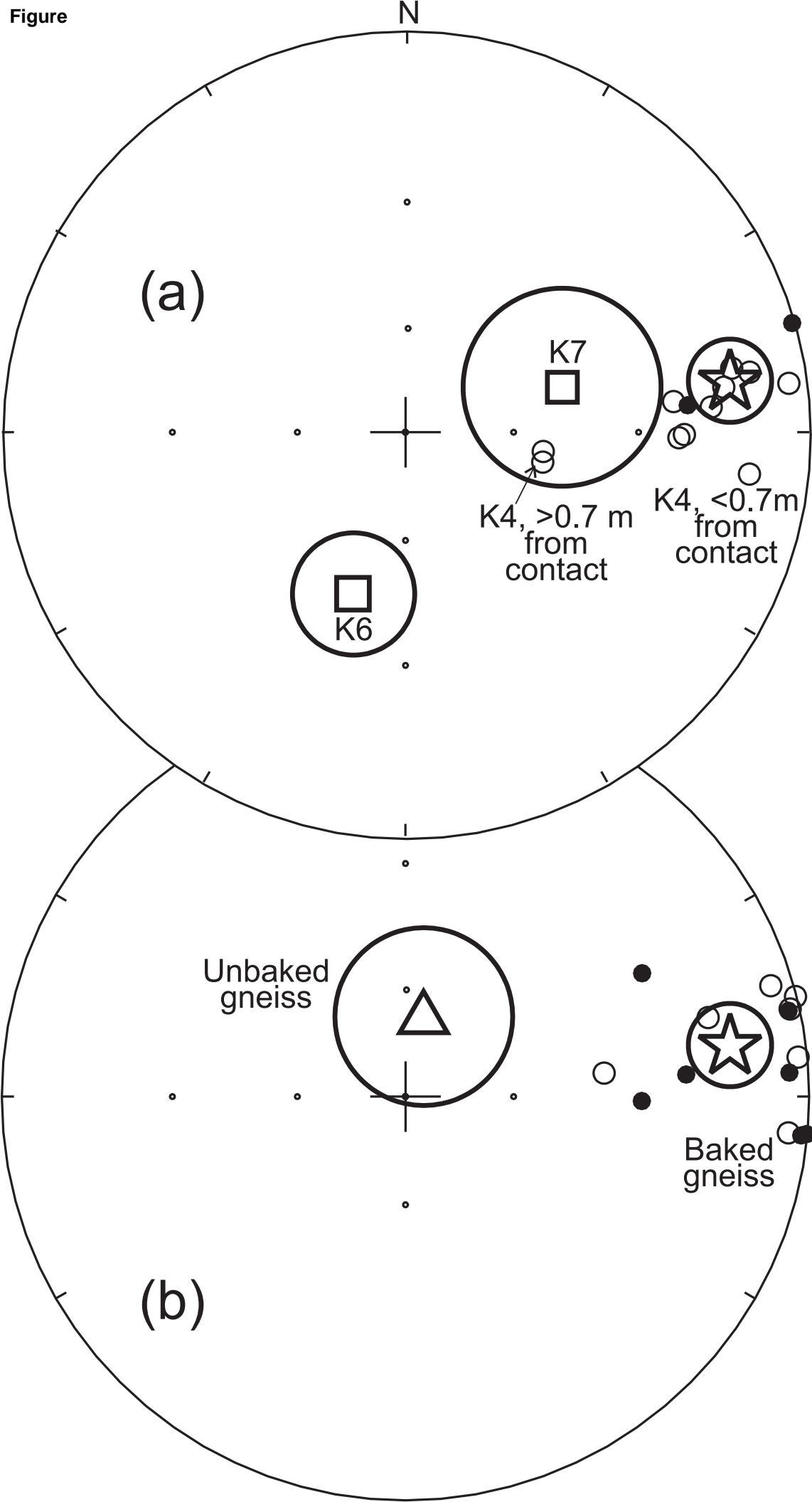


K5-12B

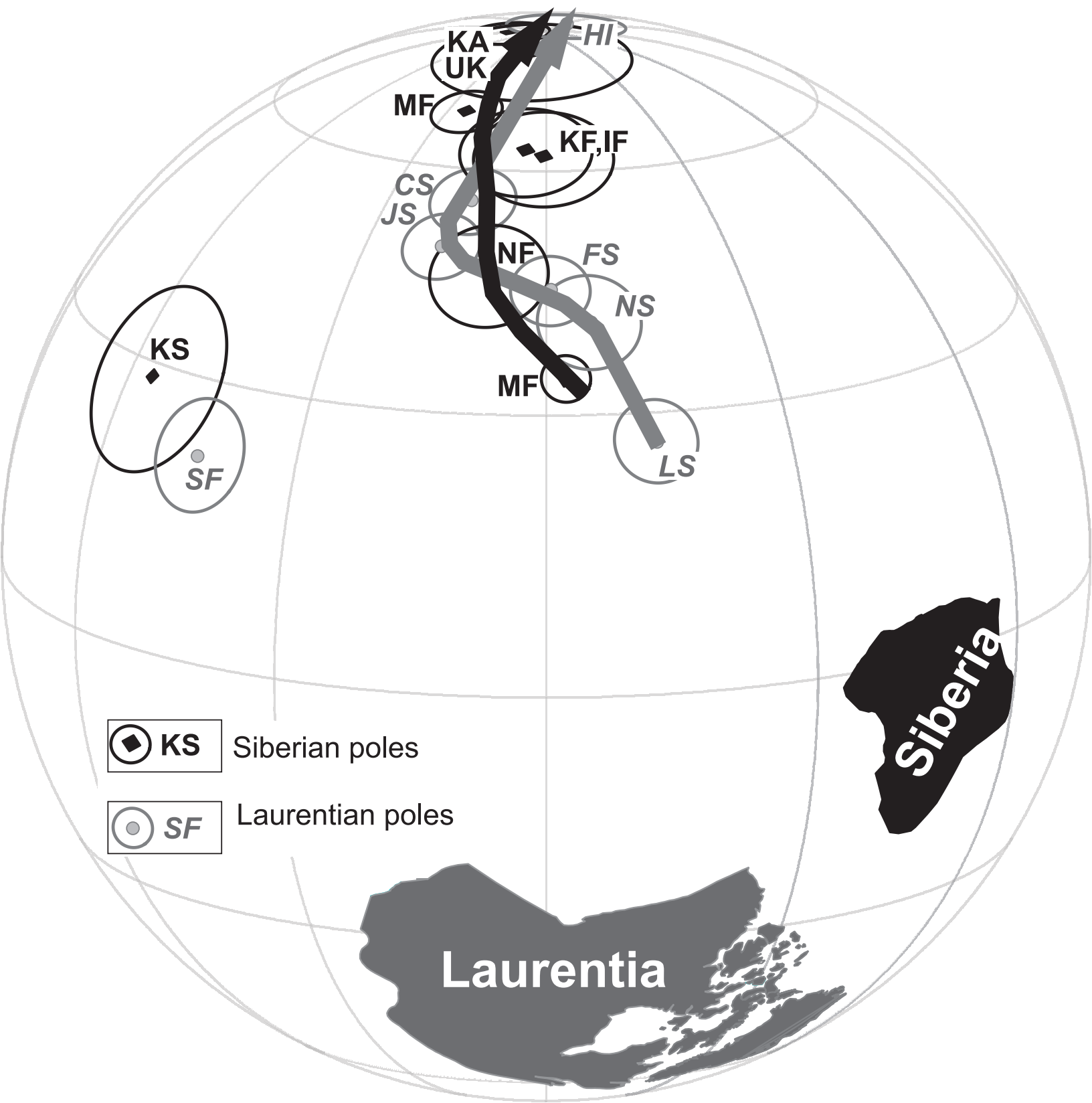


(d)

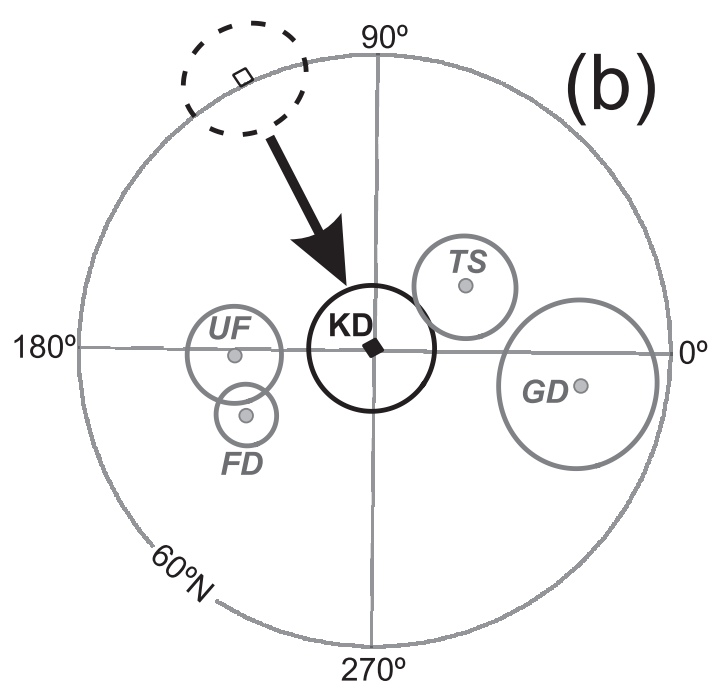
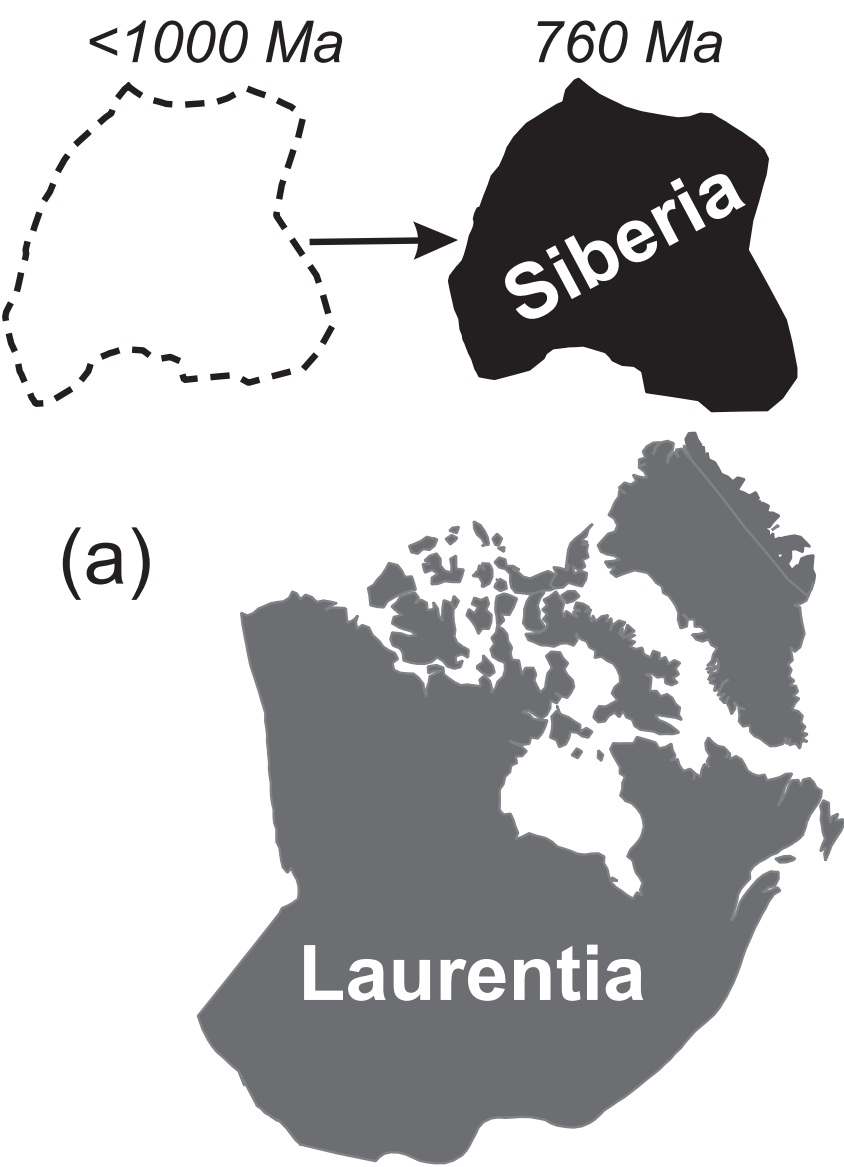
Figure



Figure



Figure



Figure

